Phase behaviour and structure of colloidal suspensions

1994 J. Phys.: Condens. Matter 6 A29

(http://iopscience.iop.org/0953-8984/6/23A/004)

J. Phys.: Condens. Matter 6 (1994) A29–A36. Printed in the UK

Phase behaviour and structure of colloidal suspensions

P N Pusey†, W C K Poon†, S M Ilett† and P Bartlett‡

† Department of Physics and Astronomy, The University of Edinburgh, Mayfield Road, Edinburgh EH9 3JZ, UK
‡ School of Chemistry, University of Bristol, Cantock's Close, Bristol BS8 1TS, UK

Received 8 November 1993

Abstract. We describe three sets of experiments on suspensions of 'hard-sphere' colloids. Suspensions of equal-sized particles exhibit the hard-sphere freezing and glass transitions. Mixtures of spheres of two different sizes can form the ordered binary crystals AB_2 and AB_{13}. The addition of non-adsorbing polymer to a one-component suspension leads, through the depletion mechanism, to a range of phase behaviour, which includes colloidal gas, liquid, crystal and gel.

1. Introduction

Colloidal suspensions consist of particles, of size typically less than 1 μm, suspended in a liquid [1]. In the theoretical description of the phase behaviour and structure of such suspensions it is usually adequate to regard the liquid as an inert thermal bath. Standard methods of thermodynamics and statistical mechanics can then be applied to the assembly of particles, which can reach thermal equilibrium through Brownian motion. At relatively low concentrations the particles form fluid-like states, showing significant short-ranged order, but in which the particles can in time diffuse throughout the sample. At higher concentrations the particles can become localized in either ordered equilibrium crystalline states or long-lived metastable 'glassy' states.

Compared to atomic or molecular matter, colloidal systems exhibit several special properties, which result mainly from the large size of the particles: typically colloids are some 1000 times larger than atoms. Colloidal solids are weak mechanically; structural relaxation times of colloidal systems are large, of order seconds. Thus a sample, initially crystalline, can be 'shear-melted' to a metastable fluid simply by shaking. Recrystallization can take minutes, hours or days, giving time for studies of both the crystallization process and the properties of the metastable states themselves. The spatial scales of colloidal systems are comparable to the wavelength of light. Light-scattering techniques are therefore powerful in studies of both structure and dynamics; for example, colloidal crystals Bragg reflect visible light. The interaction between colloidal particles can frequently be adjusted, or 'tailored', by various means such as the addition of electrolyte or free polymer to the suspension or modification of the surface coatings of the particles.

Over the last few years it has been appreciated that these special properties allow one to perform experiments with colloidal systems which, though desirable, are not possible with atomic systems. Our main motivation for colloid research might therefore be called 'colloids as atoms' [1]. A second motivation is, of course, the importance of colloidal systems in industrial products; paints, foods, pharmaceuticals etc.

0953-8984/94/SA0029+08$19.50

The particles used in the experiments described here consist of spherical 'cores' of amorphous polymethylmethacrylate (PMMA), stabilized sterically by thin chemically grafted layers of another flexible polymer, poly-12-hydroxystearic acid [2]. Particle radii ranged from 0.2 to 0.5 μm; the relative standard deviation of the size distribution of any single preparation of particles was typically less than 0.05. For most of the studies the particles were suspended in mixtures of two liquids, decahydronaphthalene (decalin) and either tetrahydronaphthalene (tetralin) or carbon disulphide, in proportions chosen to nearly match the refractive index, $\sim$ 1.50, of the particles, providing transparent samples suitable for both direct observation and light scattering. A body of circumstantial evidence suggests that there is essentially no interaction between a pair of suspended PMMA particles until, on close approach, their polymer coatings overlap; a strong repulsion resulting from compression of the coatings then comes in over a small reduction of the centre-to-centre separation. To a good approximation, then, these particles interact like hard spheres.

Assemblies of hard spheres have played an important role as simple theoretical models for the states of matter, but, because hard-sphere atoms do not exist, hard-sphere systems have been until recently inaccessible to experiment. In this paper, under three headings, we describe experimental studies of suspensions of hard-sphere PMMA colloids. *Suspensions of equal-sized PMMA colloids* show the hard-sphere freezing transition and, at higher concentrations, glass formation. *Binary mixtures* of PMMA colloids of different sizes can form the ordered binary crystals, or superlattice structures, AB_2 and AB_{13}. *Mixtures of colloids and free polymer* exhibit a range of interesting phenomena resulting from the so-called depletion attraction. In particular the effect on the phase behaviour of an assembly of particles caused by varying the range of the attraction between them can be studied. The older work under the first two headings will be described only briefly, with reference to the literature. The recent studies of colloid–polymer mixtures will be treated in more detail.

2. Suspensions of equal-sized hard-sphere colloids

The phase behaviour of an assembly of hard spheres of radius R is determined by a single variable, the volume or packing fraction $\phi = \rho\frac{4}{3}\pi R^3$, where ρ is the number density. The freezing transition of hard spheres was first observed in the early computer simulations of Alder and Wainwright [3]. Subsequent more detailed simulations by Hoover and Ree [4] established the freezing and melting concentrations to be $\phi_F = 0.494$ and $\phi_M = 0.545$. For $\phi \leqslant \phi_F$ the state of the system is fluid. For $\phi_F \leqslant \phi \leqslant \phi_M$ the equilibrium state is a coexistence of fluid and crystal, whereas for $\phi_M \leqslant \phi \leqslant \phi_{CP}$ the state is fully crystalline; here $\phi_{CP} = 0.74$ is the volume fraction of a fully-compressed close-packed crystal. Later Woodcock [5] showed, again by simulation, that, on compressing hard spheres rapidly enough to bypass crystallization, a long-lived metastable glassy state was formed at a glass transition concentration $\phi_G \sim 0.58$ and persisted up to random close packing at $\phi_{RCP} \sim 0.64$.

In 1986 experimental studies of PMMA suspensions confirmed this predicted phase behaviour, clearly identifying both the freezing and glass transitions [6]. Later experiments by 'light powder crystallography' [7] showed that the structure of the crystals was neither of the common close packings, face-centred cubic or hexagonal close-packed, but 'random-stacked close-packed'; thus an ...AB stacking of hexagonally arranged layers could be followed, with almost equal probability, by a layer in either the A or C position. Studies by dynamic light scattering [8] of the diffusive motions of the particles in both metastable fluid and glassy states have provided significant confirmation of the predictions of mode-coupling theories of the glass transition in simple systems.

In the early days of liquid-state research the very existence of the freezing transition of hard spheres was the subject of vigorous debate [9], since it contradicts the intuition that crystals are held together by attractive forces. It seems to be accepted now that the transition is driven entropically [10]: crystallization occurs at a concentration at which the configurational entropy lost when a metastable fluid becomes ordered is offset by the 'free-volume' entropy gained by the particles from the greater freedom that they have for local motions in an ordered structure.

3. Binary mixtures of hard-sphere colloids

Mixtures of large spheres A and small spheres B offer a large parameter space. In principle any size ratio R_B/R_A can be chosen; then both the ratio ρ_B/ρ_A of number densities and total volume fraction $\phi_A + \phi_B$ can be varied. Here we limit the discussion to experiments performed at size ratio $R_B/R_A \sim 0.58$, which were motivated by the following.

Remarkably the first examples of colloidal superlattices (AB_2 and AB_{13}) were found at size ratio $R_B/R_A \sim 0.58$ by Sanders [11] in naturally occurring gem opals, solidified arrays of colloidal silica spheres. To explain these observations Murray and Sanders [12] argued that superlattices whose total concentration when fully compressed is greater than that of a fully compressed one-component crystal, i.e. $\phi_A + \phi_B > 0.74$, should be stable compared to phase-separated crystals of pure A and pure B. By analogy with the freezing of equal-sized spheres, such structures should have large free-volume contributions to their entropy at the lower concentrations $\phi_A + \phi_B \sim 0.55$, at which crystals are first formed. Based on this criterion Murray and Sanders identified the observed structures, AB_2 and AB_{13}, as the only stable superlattices expected at $R_B/R_A \sim 0.58$.

In experiments [13] PMMA particles of sizes $R_B = 0.186$ μm and $R_A = 0.321$ μm ($R_B/R_A \sim 0.58$) were used. Samples were prepared at various number ratios at total concentrations in the range $0.50 \leqslant \phi_A + \phi_B \leqslant 0.55$. Both the superlattices, AB_2 and AB_{13}, were indeed observed. The structures (figure 1) were identified both by light powder crystallography performed on the suspensions and by scanning electron microscopy of particle compacts dried by slow evaporation of the liquid. Details are given in the caption to figure 1. Crystallization of both superlattices was much slower than that of the one-component suspensions, taking weeks or months rather than hours. Surprisingly the more complex AB_{13} structure crystallized significantly faster than AB_2. Indeed the latter did not crystallize at all at the stoichmetric number ratio $\rho_B/\rho_A \sim 2$, but only from metastable fluid mixtures with $\rho_B/\rho_A \sim 4$ and 6.

Largely confirming the simple ideas of Murray and Sanders, subsequent calculations, based on computer simulation [14] and density-functional theory [15], have established that the AB_2 and AB_{13} structures of hard spheres are thermodynamically stable over a range of size ratios encompassing $R_B/R_A = 0.58$. Eldridge *et al* [16] have compared their theoretical phase diagram for hard-sphere mixtures at $R_B/R_A = 0.58$ with that found experimentally [13]. While overall agreement between experiment and theory is reasonable, there are significant differences of detail. Aside from experimental and computational uncertainties, factors contributing to these differences probably include glass formation, preventing the attainment of equilibrium, and the possibility that metastable crystalline states, rather than the equilibrium states, occur for kinetic reasons.

It is clear that systems as simple as a mixture of hard spheres can self-assemble into quite complex structures, driven purely by entropic contributions to their free energies.

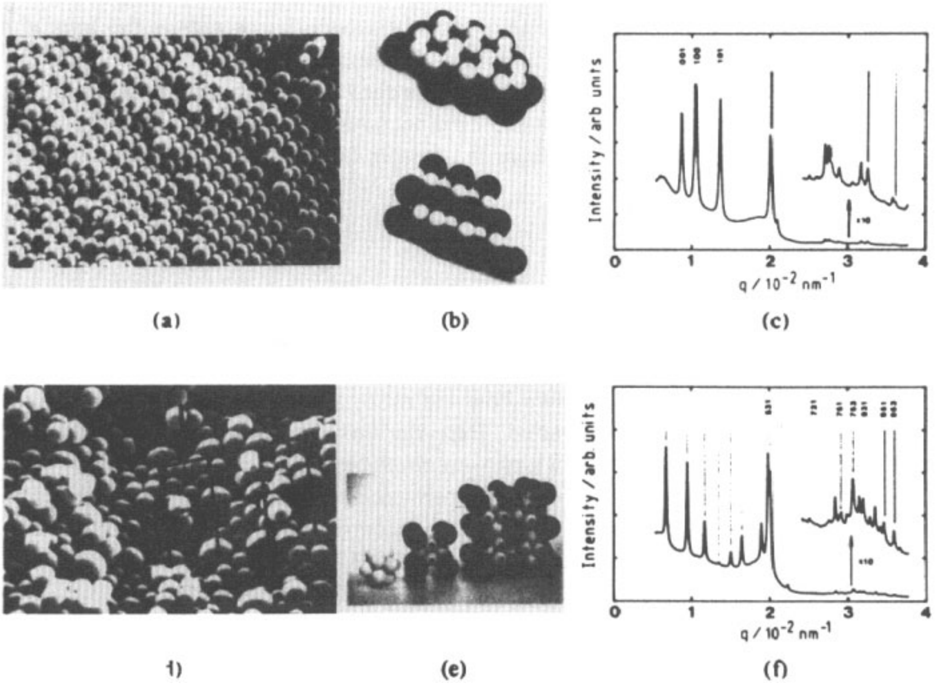

Figure 1. (*a*) Scanning electron micrograph of the 011 plane of AB_2 colloidal crystals; (*b*) the AB_2 structure, consisting of a simple hexagonal arrangement of large particles interleaved by layers of the smaller particles; (*c*) light powder diffraction pattern of AB_2, consistent with the structure shown in (*b*); (*d*) electron micrograph of AB_{13}; the grid marks large spheres from the 011 face; below the arrows, pentagons of small spheres, resulting from cleavage of the icosahedra, can be seen; (*e*) the unit cell of AB_{13} (right), composed of a simple cubic lattice of large particles; each cubic subcell contains 13 small particles, the outer 12 arranged on the vertices of an icosahedron; the icosahedra are rotated by 90° between adjacent cubic subcells; (*f*) diffraction pattern of AB_{13}; the reflections marked with odd indices are superlattice lines, which confirm the existence of the large unit cell. (Taken from [13].)

4. Mixtures of colloids and free polymer

Flexible non-adsorbing polymer molecules in a suspension of solid particles cannot penetrate the surfaces of the particles. Their centres are thus excluded from 'depletion zones', centred on the particles, of radius $R + \delta$, where δ is a measure of the polymer's radius. In a dilute system this 'depletion mechanism' has little effect. However, at higher total concentrations of colloid and polymer, it can induce a separation of the suspension into colloid-rich and colloid-poor phases. Two views can be taken of this process. Overlap of the depletion zones of different particles, particularly in the colloid-rich phases, provides more accessible, or free, volume for the polymer molecules in the sample as a whole. Thus phase separation can maximize entropy. Alternatively (but equivalently), polymer molecules are excluded from the overlapping depletion zones of two closely-spaced particles but can approach the remainder of the surfaces of the particles [17, 18]. This results in a net osmotic force, which pushes the particles together and which, if strong enough, can induce phase separation. A useful feature of the 'depletion potential' [17, 18], the effective pair potential giving rise to this attraction, is that its *depth* is determined by the concentration of polymer and its *range* by the size of the polymer. Thus, by varying the polymer concentration and the ratio of polymer to particle sizes, it is possible to investigate experimentally how the phase behaviour of an assembly of particles depends upon the nature of their interaction.

The expected phase behaviour of a colloid–polymer mixture can be calculated by adopting either of the pictures mentioned above. In 1983 Gast *et al* [19] calculated free energies by regarding the depletion potential as a perturbation to the bare colloid–colloid potential. Recently Lekkerkerker *et al* [20] applied an approximate statistical mechanical approach, modelling the system as a mixture with non-additive interactions. Thus the particles interact like hard spheres with interaction diameter $2R$, the colloid–polymer interaction is assumed to be of hard-sphere type with interaction diameter $R + \delta$, but the polymer molecules themselves are taken to be totally interpenetrable so that their self interaction has diameter zero. For the case of hard-sphere colloids and ideal polymers, both approaches give similar predictions; the results of figure 2(*a*)–(*c*) are from Lekkerkerker's approach.

Concerning the polymer concentration, it turns out that the natural variable of the theory [20] is c_{pr}, (the mass of polymer)/(the *free* volume available to the polymer), the latter being that part of the suspension's volume not occupied by the particles and their associated depletion zones; c_{pr} is related to the chemical potential of the polymer, which must be the same in coexisting phases. On the other hand the natural variable of experiment is simply c_{p}, (the mass of polymer)/(the *total* volume of the sample). Therefore we show phase diagrams in both the ϕ–c_{pr} representation, for discussion, and the ϕ–c_{p} form, for comparison with experiment (as before, ϕ is the colloid volume fraction).

Figure 2(*a*)–(*c*) shows predicted phase diagrams in the ϕ–c_{pr} plane for three values, 0.08, 0.33 and 0.57, of the ratio δ/R of polymer to particle radii, corresponding to effective attractions of different ranges. In all cases, with no added polymer ($c_{\mathrm{pr}} = 0$) one sees the fluid–solid freezing transition, discussed in section 2, of a one-component hard-sphere assembly. Even at low colloid concentration the addition of enough polymer leads to phase separation, the nature of which depends on δ/R. For $\delta/R \leqslant 0.33$, the addition of polymer leads simply to a strong broadening of the fluid–crystal coexistence region. However, for $\delta/R \geqslant 0.33$ the phase diagram takes on a different form, showing the analogues of both a gas–liquid critical point and a triple line of gas–liquid–crystal coexistence. When making a comparison between colloidal and atomic systems, c_{pr} can be regarded as playing the rôle of the inverse of temperature: thus inverting figure 2(*c*) reveals the familiar temperature–density projection of the phase diagram of an atomic material. It is found that the critical point and the triple line approach each other as δ/R is decreased, resulting in a decreasing region of stable liquid, until at $\delta/R < 0.33$ the phase diagram crosses over to the simpler form of figure 2(*a*), which shows no stable liquid.

Figure 2(*d*)–(*f*) shows the results of translating the theoretical ϕ–c_{pr} phase diagrams of figures 2(*a*)–(*c*) into the experimentally accessible ϕ–c_{p} representation. For $\delta/R = 0.08$ the main difference is that the tie lines become oblique, representing the partitioning of the polymer between the phases. In a phase with high colloid concentration, only a small free volume is available to the polymer, so a small value of c_{p} corresponds to a large value of c_{pr}. For $\delta/R \geqslant 0.33$, a new feature emerges: the triple *line* of the ϕ–c_{pr} representation becomes a triangular *region* of three-phase coexistence in the ϕ–c_{p} plane. At $\delta/R \sim 0.33$ the region of gas–liquid coexistence is infinitesimally small.

The samples used in our experiments comprised PMMA colloids of radius $R = 0.23$ μm suspended in *cis*-decalin and polystyrene polymer of three different molecular weights, 3.9×10^5, 2.85×10^6 and 1.44×10^7. The polystyrene/*cis*-decalin system has been characterized thoroughly [21]; if the interaction radius δ of the polymer is identified with

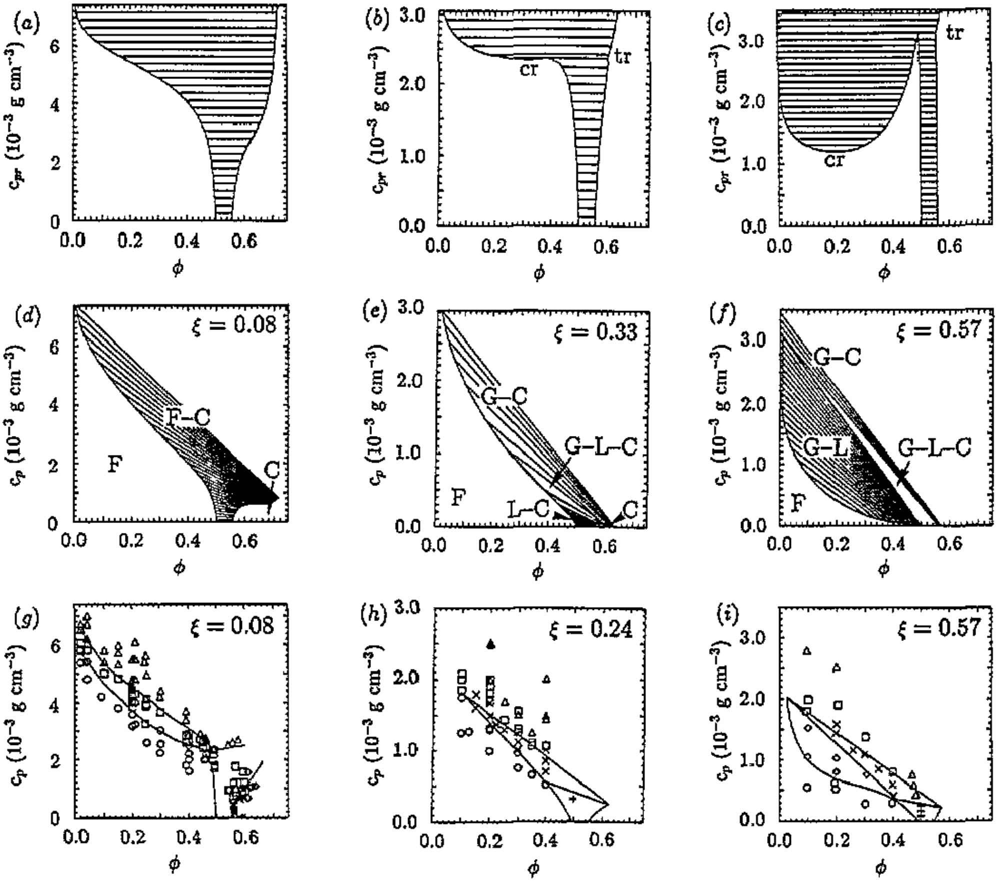

Figure 2. (*a*)–(*c*) Predicted phase diagrams in the ϕ–c_{pr} representation for polymer/particle size ratios ($\xi = \delta/R$) of 0.08, 0.33 and 0.57 (ϕ is the colloid volume fraction and c_{pr} the concentration of polymer in the free volume available to it). In (*a*) only fluid, fluid + crystal and crystal are predicted. In (*c*) a region of gas–liquid coexistence is also predicted; the critical point and triple line are indicated. In (*b*) the critical point and triple line almost coincide. (*d*)–(*f*) Theoretical phase diagrams of (*a*)–(*c*) translated into the experimentally accessible ϕ–c_p representation, where c_p is the polymer concentration in the sample. Note that the triple lines of (*b*) and (*c*) have become triangular triple regions of three-phase coexistence in (*e*) and (*f*). F denotes fluid, C, crystal, G, gas and L, liquid. The compositions of the phases in the triangular regions are given by the vertices of the triangle: left-hand vertex, gas; right-hand vertex, crystal; middle vertex, liquid. (*g*)–(*i*) Experimental results for comparison with (*d*)–(*f*): circles, one-phase fluid; squares, fluid (or gas) + crystal; crosses, gas + liquid + crystal; diamonds, gas + liquid; triangles, gel. Estimated phase boundaries are drawn to guide the eye; the upper line in (*g*) represents the gel boundary.

its radius of gyration, the size ratios of our samples correspond to $\delta/R = 0.08, 0.24$ and 0.57.

The results of visual observation of a large number of samples, after preparation and thorough mixing, are shown in figure 2(*g*)–(*i*). At $\delta/R = 0.08$ and $\phi < 0.49$, the addition of a relatively small amount of polymer provided samples that remained in a single phase for some days. Addition of more polymer led to phase separation within hours. Small crystallites, identified by visible Bragg reflections, appeared throughout the samples and settled under gravity to form well defined polycrystalline layers [22]. At $\delta/R = 0.57$, samples in the gas–liquid coexistence regions developed slightly diffuse boundaries, appearing near the top and subsequently moving down, which separated two amorphous phases, a quite opaque lower phase and a less cloudy upper phase. In the three-phase region, crystallites formed throughout the samples within a few hours and, at about the same time, the gas–liquid boundary appeared. After a day or two, three-phase coexistence was clearly evident, the middle liquid phase being separated from the polycrystal at the bottom by a sharp interface and from the upper gas by a more diffuse interface. At $\delta/R = 0.24$, while a significant area of three-phase coexistence was observed, the two-phase gas–liquid region was very narrow. Thus, experimentally, the size ratio at crossover between the two generic types of phase behaviour seems to be around $\delta/R = 0.24$. Finally, we mention that the addition of polymer in significant excess of that required to provide phase separation led in all cases to the formation of apparently metastable 'colloidal gels', discussed elsewhere [23].

Regarding the topology of the diagrams there is reasonable agreement between experiment and theory, although the observed value, ~ 0.24, of the size ratio at crossover between the two types of phase behaviour is significantly smaller than that, 0.33, predicted. However there are noticeable differences between the experimental and theoretical positions of the phase boundaries. These are probably the result of approximations in the theoretical model [20], particularly the mean-field approach and the idealized treatment of the polymer.

As mentioned above, when cast in terms of the theoretically relevant variable c_{pr}, the approaches of both Gast *et al* [19] and Lekkerkerker *et al* [20] predict similar phase behaviour. However the second approach leads more transparently to phase diagrams that can be compared directly with experiment and which display explicitly the partitioning of polymer between the various phases. Indeed, in the 1980s, the fact that comparison was made between experiment presented in terms of c_{p} and theory in terms of c_{pr} led to some confusion. A striking difference between the two representations is that in the ϕ–c_{pr} plane three-phase coexistence is seen only on the triple *line* whereas in the experimental ϕ–c_p representation one finds a triangular three-phase *region*. Three-phase coexistence in colloid-polymer mixtures has also been reported recently by Leal Calderon *et al* [24], who studied a mixture of charged polystyrene colloids and hydroxyethyl cellulose polyelectrolyte and sketched phase boundaries similar to those of figure 2(i)–(g) (but without showing data points).

We conclude with a comment of broader relevance. The phase diagrams of figure 2(a)–(c) suggest that an assembly of particles will only show a gas–liquid critical point, and a stable liquid phase, if the range of their attraction is greater than about 20–30% of their diameter. One might guess this to be a general result, applicable to molecular systems and not specific only to a potential of the depletion form. This implication of the 1983 calculations of Gast *et al* [19] appears to have been largely overlooked by the traditional liquids community [25], although Stell [26] has discussed the extreme case of a deep narrow attraction, 'sticky hard spheres'. Also in this connection, recent theoretical studies of the phase behaviour of C_{60}, large molecules with relatively short-ranged attractions, find either a very narrow liquid region [27] or no liquid at all [28].

Acknowledgments

We thank Dr W van Megen and Professor R H Ottewill for collaboration on some of the work mentioned in this paper, Professor H N W Lekkerkerker for many valuation discussions and

S Erbil, A Orrock, A D Pirie, M B Robertson, J S Selfe and M K Semmler for assistance in determining the colloid–polymer phase diagrams. Parts of the research reported here were funded by the SERC, the AFRC and the MOD.

References

[1] Pusey P N 1991 *Liquids, Freezing and the Glass Transition, Les Houches Session LI* ed D Levesque, J-P Hansen and J Zinn-Justin (Amsterdam: North-Holland) p 763

[2] Antl L, Goodwin J W, Hill R D, Ottewill R H, Owens S M, Papworth S and Waters J A 1986 *Colloid Surf.* **17** 67

[3] Alder B J and Wainwright T E 1957 *J. Chem. Phys.* **27** 1208

[4] Hoover W G and Ree F H 1968 *J. Chem. Phys.* **49** 3609

[5] Woodcock L V 1981 *Ann. N Y Acad. Sci.* **37** 274

[6] Pusey P N and van Megen W 1986 *Nature* **320** 340

[7] Pusey P N, van Megen W, Bartlett P, Ackerson B J, Rarity J G and Underwood S M 1989 *Phys. Rev. Lett.* **63** 2753

[8] van Megen W and Pusey P N 1991 *Phys. Rev.* A **43** 5429
van Megen W and Underwood S M 1993 *Phys. Rev. Lett.* **70** 2766

[9] Percus J K (ed) 1963 *The Many-Body Problem* (New York: Wiley–Interscience) p 497

[10] Frenkel D 1993 *Phys. World* **6** 24 and this volume
Ackerson B J 1993 *Nature* **365** 11

[11] Sanders J V 1980 *Phil. Mag.* A **42** 705

[12] Murray M J and Sanders J V 1980 *Phil. Mag.* A **42** 721

[13] Bartlett P, Ottewill R H and Pusey P N 1992 *Phys. Rev. Lett.* **68** 3801; 1990 *J. Chem. Phys.* **93** 1299

[14] Eldridge M D, Madden P A and Frenkel D 1993 *Mol. Phys.* **79** 105; 1994 *Mol. Phys.* at press

[15] Xu H and Baus M 1992 *J. Phys.: Condens. Matter* **4** 663

[16] Eldridge M D, Madden P A and Frenkel D 1993 *Nature* **365** 35

[17] Asakura S and Oosawa F 1954 *J. Chem. Phys.* **22** 1255; 1958 *J. Polym. Sci.* **33** 183

[18] Vrij A 1976 *Pure Appl. Chem.* **48** 471

[19] Gast A P, Hall C K and Russel W B 1983 *J. Colloid Interface Sci.* **96** 251

[20] Lekkerkerker H N W, Poon W C K, Pusey P N, Stroobants A and Warren P B 1992 *Europhys. Lett.* **20** 559

[21] Berry G C 1966 *J. Chem. Phys.* **44** 4550

[22] The phase diagram at $\delta/R = 0.08$, figure 2(*g*), has been described in detail by
Poon W C K, Selfe J, Robertson M, Ilett S M, Pirie A D and Pusey P N 1992 *J. Physique* II **3** 1075

[23] Pusey P N, Pirie A D and Poon W C K *Physica* A at press

[24] Leal Calderon F, Bibette J and Biais J 1993 *Europhys. Lett.* **23** 653

[25] See, however, [1] p 805.

[26] Stell G 1991 *J. Stat. Phys.* **63** 1203

[27] Cheng A, Klein M L and Caccamo C 1993 *Phys. Rev. Lett.* **71** 1200

[28] Hagen M H J, Meijer E J, Mooij G C A M, Frenkel D and Lekkerkerker H N W 1993 *Nature* **365** 425